Bioorganic Chemistry 88 (2019) 102932

Contents lists available at ScienceDirect

Bioorganic Chemistry

journal homepage: www.elsevier.com/locate/bioorg

# Design, synthesis and photoinduced DNA cleavage studies of [1,2,4]-triazolo [4,3-*a*]quinoxalin-4(5*H*)-ones

Garima Sumran[a,*], Ranjana Aggarwal[b], Ashwani Mittal[c], Aviral Aggarwal[d], Amit Gupta[e]

[a] Department of Chemistry, D. A. V. College (Lahore), Ambala City 134 002, Haryana, India
[b] Department of Chemistry, Kurukshetra University, Kurukshetra 136 119, India
[c] Biochemistry Department, University College, Kurukshetra University, Kurukshetra 136 119, India
[d] Birla Institute of Technology and Science, Pilani-K. K. Birla Goa Campus, Goa 403 726, India
[e] Department of Chemistry, Dronacharya Government College, Gurgaon 122 001, India

ARTICLE INFO

*Keywords:*
Triazolo[4,3-*a*]quinoxalin-4(5*H*)-ones
Iodobenzene diacetate
Supercoiled plasmid
Superoxide anion radical
Photocleavage
AM1 calculations

ABSTRACT

An expedient and eco-friendly synthesis of 1-aryl/heteroaryl-[1,2,4]-triazolo[4,3-*a*]quinoxalin-4(5*H*)-ones (**4**) has been accomplished *via* iodobenzene diacetate mediated oxidative intramolecular cyclization of 3-(2-(aryl/heteroarylidene)hydrazinyl)-quinoxalin-2(1*H*)-ones (**3**). Ten synthesized compounds **3** and **4** (10–40 μg) on irradiation with UV light at $\lambda_{max}$ 312 nm could lead to cleavage of supercoiled pMaxGFP DNA (Form I) into the relaxed DNA (Form II) without any additive. Further, DNA cleaving ability of triazoles was quantitatively evaluated and was found to be dependent on its structure, concentration, and strictly on photoirradiation time. Mechanistic investigations using several additives as potential inhibitors/activator revealed that the DNA photocleavage reaction involves Type-I pathway leading to formation of superoxide anion radicals ($O_2^{-\cdot}$) as the major reactive oxygen species responsible for photocleavage process.

## 1. Introduction

For many decades, interaction between small organic molecules preferably heterocyclic based compounds and DNA has been a subject of intensive investigation with the perspective of development of new DNA targeting antitumor drugs *viz.* bleomycins, Hoechst 33258, doxorubicin, amsacrine, cisplatin, phenanthriplatin [1–4]. In this context, photonucleases embrace vast promise in genomic research and medicinal chemistry due to their ability to cause significant damage on DNA with or without site selectivity upon irradiation by ultra-violet or visible light [5,6]. Furthermore, the organic compound is not consumed in the process. Photonucleases comprise multifarious potential in the design and development of synthetic restriction enzymes, as sequence-specific cleavage agents [7,8], as molecular probes that can recognize specific DNA sequences [9,10], as DNA footprinting agents to study DNA-drug and DNA-protein interactions [11], as pharmacological and therapeutic agents [12–14] as well. Additionally, they find promising utility as highly targeted photochemotherapeutic agents and in photodynamic therapy (PDT) for cancerous or non-malignant tissues [15–18].

Triostin A, tandem and azatriostin are members of quinoxaline family of antibiotics that have strong DNA-binding and potential antitumor activity [4]. In fact, the activity of antiviral indolo[2,3-*b*]quinoxaline derivatives also finds its origin in interactions with DNA [19]. It has been observed that DNA binding and/or topoisomerase II inhibition contribute to cytotoxicity of [1,2,4]-triazolo[4,3-*a*]quinoxaline derivatives against three tumor cell lines namely HePG-2, Hep-2 and Caco-2 [20]. Peptide derivatives of 3-(quinoxalin-6-yl)alanine are also known to cause oxidative DNA damage in combination with Cu(II) or Fe(II) ions [21]. Additionally, many 1,2,3-triazole derivatives have exhibited antitumor or DNA photocleavage activities [22–24]. 1,2,4-Triazole-based copper(II) complex has been reported to possess nuclease activity [25]. Despite this, potential of triazoloquinoxalines as photonucleases is poorly explored. The study of quinoxaline and triazole pharmacophores endowed with the ability to photocleave DNA in presence of cofactors can be envisioned to provide a rational basis for the design and synthesis of new photonucleases by fusing electron rich triazole ring to 1,2-bond of the quinoxaline ring to extend the planarity of the system. Since metal-based photosensitizers possess certain limitations like solubility, side effects, intrinsic and extrinsic resistance, therefore, design of photonucleases which functions without any additives such as metals and reducing agents is highly enviable. Accordingly, we have previously reported synthesis of 1-aryl/heteroaryl-4-methyl-1,2,4-triazolo[4,3-*a*]quinoxalines **I** and their potential of

* Corresponding author.
*E-mail address:* garimasumran@gmail.com (G. Sumran).

https://doi.org/10.1016/j.bioorg.2019.102932
Received 4 September 2018; Received in revised form 20 March 2019; Accepted 15 April 2019
Available online 19 April 2019
0045-2068/ 

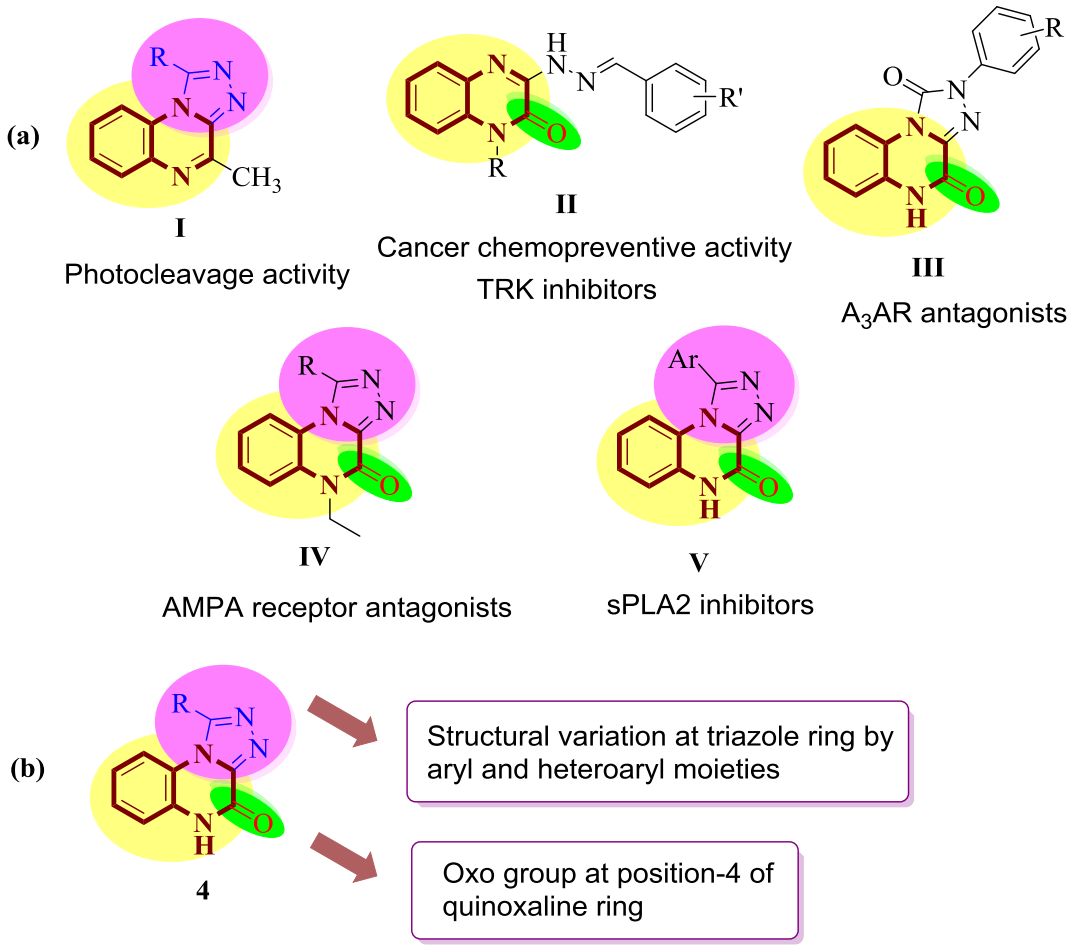


**Fig. 1.** (a) Structures of previously reported biologically active quinoxaline derivatives (**I–V**). (b) The proposed [1,2,4]-triazolo[4,3-*a*]quinoxalin-4(5*H*)-ones (**4**) in the present study.

photocleaving supercoiled plasmid ΦX174 DNA from Form I to II [26] (Fig. 1a). Literature precedent indicated that hydrazone derivatives of quinoxalin-2(1*H*)-ones **II** are reported as cancer chemopreventive agents with potent and selective inhibition of tyrosine kinase (TRK) receptor [27] and 1,2,4-triazolo[4,3-*a*]quinoxalin-4(5*H*)-one derivatives **III**, **IV** act as potent and/or selective antagonists of several receptors such as $A_3$ adenosine [28] and AMPA receptor [29]. In addition, 1-(substituted-phenyl)-5*H*-[1,2,4]-triazolo[4,3-*a*]quinoxalin-4-ones **V** have exhibited inhibitory effect on secreted phospholipase A2 (sPLA2) [30]. Moreover, 1,2,4-triazolo[4,3-*a*]quinoxalin-4(5*H*)-one derivatives act as important template for the selective construction of diverse heterocyclic scaffolds of synthetic and biological importance [29,31]. Keeping in view the bio-active profile of triazoloquinoxalines and as a part of our continuing research directed toward the unique applications of iodobenzene diacetate (IBD) in synthetic organic transformations [32–34], we wish to report herein a convenient synthesis and DNA photocleavage activities of some [1,2,4]-triazolo[4,3-*a*]quinoxalin-4(5*H*)-ones (**4**) having structural modification at position-4 of compound **I**.

## 2. Designing based on molecular orbital calculations

In the quest for designs of more active DNA photocleavers, it is an effective strategy to incorporate new functional groups or structural modifications. In the present work, rationale was to study whether the replacement of methyl substituent at 4th position of reported photonucleases **I** with oxo group in triazolo[4,3-*a*]quinoxalin-4(5*H*)-one derivatives **4** (Fig. 1b), would lead to subtle or substantial changes in DNA photocleavage activity. Oxo group was introduced so as to impart various electronic and lipophilic or hydrogen bond accepting properties to the target molecules that might contribute to the enhancement of DNA photocleavage activity.

The initial geometry optimization of compounds **4a, b**, **i-k** were performed using molecular mechanics method and MM+ force field, where the minimum energy conformations are obtained (Fig. S1, Supporting Information). These conformations were used further for single point level calculations. The minimum energy in the most stable conformation, lowest unoccupied molecular orbital (LUMO) and highest occupied molecular orbital (HOMO) energies for compounds **4a**, **b**, **i-k** were obtained from AM1 force field semi-empirical quantum calculations, using molecular modeling programs HyperChem 7.0 and are listed in Table 1. The simulated electron densities distribution of HOMO and LUMO of these compounds are shown in Fig. S2 (Supporting Information).

Dong et al reported that DNA photocleavage efficiency is directly related to the energy gap between LUMO and HOMO ($\Delta E_{L\text{-}H}$) of isomeric methylbenz[*a*]anthracenes [35]. Therefore, it was envisaged in the present study to incorporate oxo group at position-4 of triazoloquinoxaline ring as it causes a slight enhancement in the HOMO-LUMO gaps in comparison with methyl substituent at position-4 of triazoloquinoxalines **I** [26]. For instance, the HOMO energy levels of **4i** can be depressed by 0.41 ev through oxo substitution in comparison to corresponding reported analog **I** [26]. Interestingly, the nature of R group also affects the energy gap. The band gaps ($\Delta E_{L\text{-}H}$) of **4a** (having unsubstituted phenyl on triazole ring) and **4j** (having unsubstituted thienyl on triazole ring) are greater than 4**b** (having 4′-fluorophenyl on

**Table 1**
The minimum energy and frontier orbitals energies for **4a, b, i-k**.

| Compd. | R | E[a] | LUMO[a] | HOMO[a] | $\Delta E_{L-H}$ |
|---|---|---|---|---|---|
| **4a** | -$C_6H_5$ | −3466.07 | −1.175433 | −9.098546 | 7.923113 |
| **4b** | -*p*-$FC_6H_4$ | −3477.74 | −1.324252 | −9.139587 | 7.815335 |
| **4i** | -2′-furyl | −3111.30 | −1.145003 | −9.27898 | 8.133977 |
| **4j** | -2′-thienyl | −3098.81 | −1.113257 | −9.207574 | 8.094317 |
| **4k** | -5′-bromo-2′-thienyl | −3070.22 | −1.299559 | −9.285626 | 7.986067 |
| **I**[b] | -2′-furyl | −3113.266902 | −1.161189 | −8.870054 | 7.708865 |
| **I**[b] | -2′-thienyl | −3117.678469 | −1.180223 | −8.947033 | 7.76681 |

[a] E (minimum energy of molecule in least strained conformation, kcal/mol) and the frontier orbital energies (ev) were obtained from AM1 force field calculations.
[b] Ref. [26].

triazole ring) and **4k** (having 5′-bromo-2′-thienyl on triazole ring), respectively. Thus, it may be presumed that the triazoloquinoxalinones proposed in present study might have better potential towards DNA cleavage as compared to earlier reported photonucleases **I** [26].

## 3. Chemistry

### 3.1. Synthesis

The precursor, quinoxalin-2,3(1*H*,4*H*)-dione **1** was synthesized by the reaction of *o*-phenylenediamine with oxalic acid in 4 N HCl. Treatment of compound **1** with 50% hydrazine hydrate furnished 3-hydrazinoquinoxalin-2(1*H*)-one (**2**) [36]. Compound **2** on condensation with various aromatic/heteroaromatic aldehydes in ethanol under reflux readily afforded the corresponding key intermediates, 3-(2-(aryl/heteroarylidene)hydrazinyl)-quinoxalin-2(1*H*)-ones (**3a-k**). Ensuing oxidative intramolecular cyclization of a variety of **3** with 1.1 equiv of IBD in dichloromethane under stirring at room temperature for 2 h resulted in the formation of 1-aryl/heteroaryl-[1,2,4]-triazolo[4,3-*a*] quinoxalin-4(5*H*)-ones (**4**) in excellent yields (Scheme 1). This method is superior than the earlier reported methods which involve pyrolysis of corresponding hydrazones in presence of high boiling solvent ethylene glycol or DMSO at 200 °C for 5–8 h [37–38] and oxidative cyclization of hydrazones using bromine in acetic acid to afford [1,2,4]-triazolo[4,3-*a*]quinoxalin-4(5*H*)-ones [30]. Unfortunately, these methods offer some limitations such as poor yields of products, harsh reaction conditions, side product formation, prolong and complex procedures, cumbersome product isolation procedures and toxic reagents. The present protocol using IBD in oxidative transformation is mild, efficient, environmentally benign and reaction times are considerably reduced. Therefore, it is better than earlier methods in terms of selectivity, ready availability and ease of handling of IBD.

Structure of the new compounds **4d**, **e**, **g**, **h**, **j** and **k** was confirmed by elemental analyses, MS and a careful comparison of their IR and NMR spectra with those of their corresponding hydrazones **3d**, **e**, **g**, **h**, **j** and **k**. The structure of the reported hydrazones **3** and triazoles **4** has been confirmed from their literature melting points. The results were summarized in Table 2.

### 3.2. Results and discussion

IR spectra of **3d**, **e**, **g**, **h**, **j** and **k** showed characteristic absorption bands at ~3155–3297 $cm^{-1}$ for N—H stretching, 1674–1682 $cm^{-1}$ for C=O of amide, besides C=N stretching bands at 1600–1620 $cm^{-1}$. The $^1$H NMR spectra of **3d**, **e**, **g**, **h**, **j** and **k** displayed a sharp singlet at $\delta$ 8.50–8.87 ppm for azomethine (—N=CH—) proton and two broad singlets at $\delta$ 11.07–11.54 and $\delta$ 12.15–12.41 ppm corresponding to resonance of NH of hydrazone and of amide, respectively, as these were exchangeable with $D_2O$. $^1$H and $^{13}$C NMR spectra of hydrazones showed their existence in geometric *E*-configuration. However, compounds **3g** and **3h** existed in two geometrical isomers. Compounds **3g** displayed —N=C—H resonance at $\delta$ 7.93 ppm (15%, *Z*-isomer) and 8.55 ppm (85%, *E*-isomer), therefore, must exist in both the *Z* and *E*-imine configuration and in agreement with literature [39]. An important characteristic feature in the $^1$H NMR spectra of **4d**, **e**, **g**, **h**, **j** and **k** was the disappearance of the signals at $\delta$ 8.50–8.87 and 11.07–11.54 corresponding to azomethine (—N=CH—) and NH, respectively, of its precursor hydrazones **3**, thus indicating the successful triazole ring formation. The disappearance of absorption band for N—H stretching in IR spectra further confirmed the structure of compounds **4d**, **e**, **g**, **h**, **j** and **k**.

The plausible mechanism for the transformation of hydrazones **3** to triazoles **4** is depicted in Scheme 2. Initial electrophilic attack of IBD on **3** gives an I(III) intermediate **A**. Subsequently, intermediate **A** undergoes reductive loss of iodobenzene along with elimination of a molecule of acetic acid to generate another intermediate, nitrile imine **B**, which finally undergoes cyclization to yield the product **4**.

## 4. Photoinduced cleavage of pMaxGFP supercoiled plasmid DNA by 3-(2-(aryl/heteroarylidene)hydrazinyl)-quinoxalin-2(1*H*)-ones (3) and [1,2,4] -triazolo [4,3-*a*] quinoxalin-4(5*H*)-ones (4)

Specifically, five triazolo[4,3-*a*]quinoxalin-4(5*H*)-ones **4a, b**, **i-k** bearing phenyl, 4′-fluorophenyl, 2′-furyl, 2′-thienyl and 5′-bromo-2′-thienyl at position-1 of triazoles were chosen, out of the eleven synthesized compounds, for preliminary DNA photocleavage studies. The choice of these compounds was made on their solubilities and on the observation that these rings play crucial role in cleaving DNA

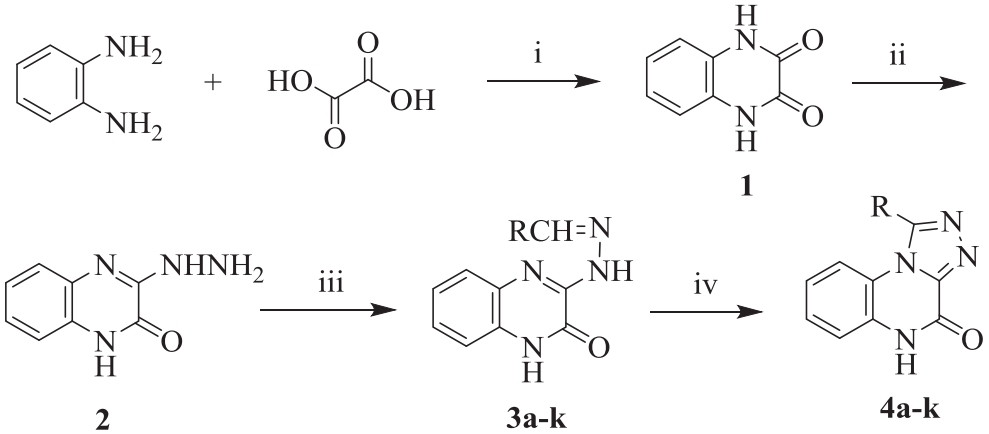


**Scheme 1.** Synthesis of 1-aryl/heteroaryl-[1,2,4]-triazolo[4,3-*a*]quinoxalin-4(5*H*)-ones (**4a-k**). Reagents and conditions: (i) 4 N HCl, reflux, 4 h; (ii) 50% $NH_2NH_2{\cdot}H_2O$, reflux, 2 h; (iii) RCHO, $C_2H_5OH$, reflux, 2 h; (iv) $PhI(OAc)_2$, $CH_2Cl_2$, stir, room temperature, 2 h.

**Table 2**
Structural substitution pattern and physical data of compounds **3a-k** and **4a-k**.

| 3,4 | Substituent (R) | Yield[a] (%) | M.p.[b]/Lit. m.p. (°C) [ref] | Yield[c] (%) | M.p.[d]/Lit. m.p. (°C) [Ref.] |
|---|---|---|---|---|---|
| **a** |  | 95 | 246/245–247 [37] | 92 | > 250/ > 300 [37] |
| **b** | 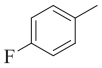 | 94 | > 250/285–287 [37] | 93 | > 250/ > 300 [37] |
| **c** | 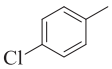 | 94 | 258/256–258 [37] | 91 | > 250/ > 300 [37] |
| **d** | 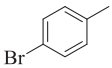 | 92 | 257–258[e] | 88 | > 310[e] |
| **e** | 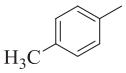 | 89 | 230–232[e] | 82 | > 320[e] |
| **f** | 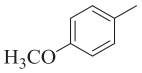 | 92 | 242/240–244 [37] | 90 | > 250/ > 300 [37] |
| **g** | 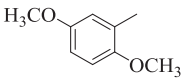 | 87 | 220–222[e] | 86 | 279–281[e] |
| **h** | 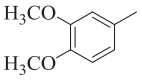 | 89 | 255–256[e] | 85 | 298–300[e] |
| **i** |  | 90 | 242/216–219 [38] | 87 | > 280/ > 360 [38] |
| **j** |  | 91 | 259–261[e] | 91 | 302–304[e] |
| **k** | 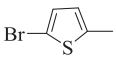 | 90 | 247–249[e] | 90 | 292–294[e] |

[a] Yield of isolated product **3**.
[b] M.p. of product **3**.
[c] Yield of isolated product **4**.
[d] M.p. of product **4**.
[e] See experimental section.

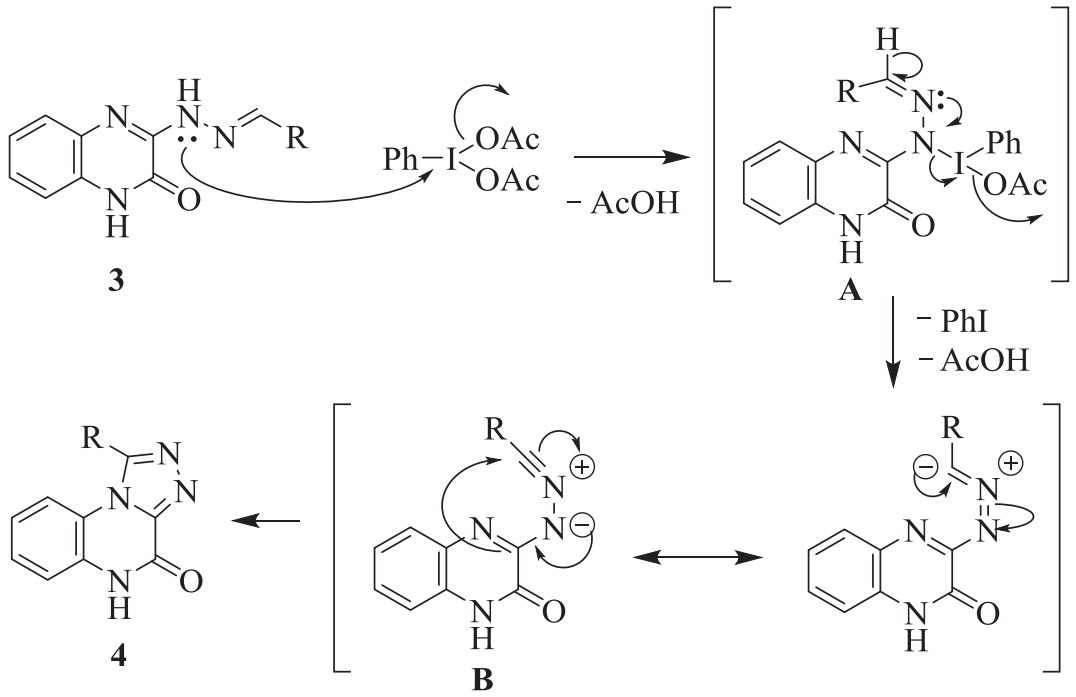


**Scheme 2.** Plausible mechanism for the transformation of hydrazones (**3**) into [1,2,4]-triazolo[4,3-*a*]quinoxalin-4(5*H*)-ones (**4**).

**Table 3**
Absorption peaks of **4a, b, i-k** in $CHCl_3$.

| Compd | $\lambda_{abs}$[a]/nm (log ε)[b] |
|---|---|
| **4a** | 305 (4.05) |
| **4b** | 305 (4.0) |
| **4i** | 308 (4.11) |
| **4j** | 306 (3.91) |
| **4k** | 308 (4.06) |

[a] Maximum absorption wavelength.
[b] Molar absorption coefficient (in $mol^{-1}\,L\,cm^{-1}$) at the maximum absorption wavelength.

photochemically [26]. It was found that the absorption wavelengths of compounds **4a, b**, **i-k** were at 305–308 nm (Table 3), which was quite close to the photoirradiation wavelength of transilluminator ($\lambda_{irr}$ 312 nm) and was not absorbed by DNA.

### 4.1. DNA photocleavage

The photocleavage activities of compounds **3a**, **b**, **i-k** and **4a**, **b**, **i-k** were evaluated quantitatively using supercoiled double-stranded pMaxGFP plasmid DNA (0.2 μg/μl) in buffer upon irradiation with UV light of 312 nm for 45 min (room temperature, pH 8.0) under aerobic conditions. The excited state of these molecules, also called photonucleases, initiate a series of damages which can lead to DNA photocleavage and photocleave products were analyzed on a 0.8% agarose gel. The gel mobility assay is sensitive to changes in DNA length or conformation. The relatively fast migration is observed for the intact supercoiled conformer (Form I) and the slower moving nicked circular conformer (Form II) generates from supercoiled DNA when scission occurs on one strand (nicking) [40].

### 4.2. Results

Fig. 2 shows gel electrophoresis separation of pMaxGFP plasmid after incubation with the compound **4** (2 μl, 30 μg) under UV irradiation. It is apparent that practically all these compounds resulted in relatively high amount of nicked DNA (Form II), which result from single strand damage (Fig. 2), indicating that [1,2,4]-triazolo[4,3-*a*]quinoxalin-4(5*H*)-one derivatives (**4**) also can be active photonucleases. Two clear bands were observed for the control DNA (lane 1, Fig. 2a and b). No obvious DNA cleavage was observed (Fig. 2a and b) for controls in which (i) DNA incubated with DMSO (2 μl) in the absence of compound **4** was left in dark (lane 2, Fig. 2b), (ii) incubation of the plasmid with DMSO (2 μl) and UV irradiation (Fig. 2a, lane 2 and Fig. 2b, lane 3), or (iii) incubation of the plasmid with **4b**, **4a**, **4i** (lane 3, 5, 7, respectively, Fig. 2a), **4j**, **4k** in dark (lane 4, 6, respectively, Fig. 2b) compared to control lane 1 (DNA alone). None of the tested compounds showed DNA cleavage in the absence of UV light (Fig. 2a, lane 3, 5, 7 and Fig. 2b, lane 4, 6), thus demonstrating the excited states of triazoloquinoxalinones are responsible for the DNA scission and ruling out any possibility of hydrolytic DNA cleavage. All experiments were performed in triplicates.

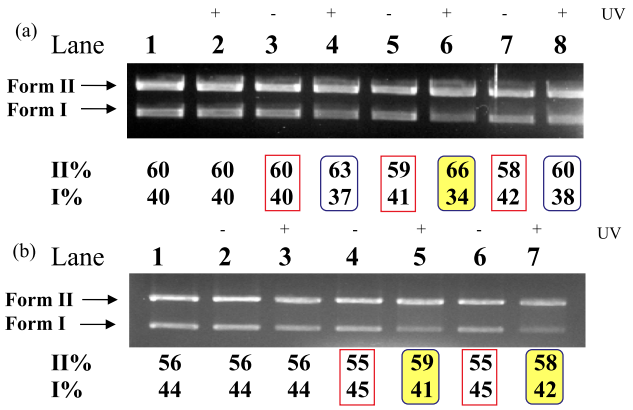


**Fig. 2.** Photocleavage of 1 μl (0.2 μg/μl) closed supercoiled pMaxGFP plasmid DNA by **4a, b**, **i-k** at concentration of 30 μg (2 μl) in DMSO (stock conc. 15 mg/mL) in TAE buffer (in 0.04 M Tris-borate, 0.114% acetic acid and 50 mM EDTA, pH 8.0). In the control lane 1, compound **4** was substituted by an equivalent volume of reaction buffer. (a) Effects of different substituents on photocleavage (photoirradiation 312 nm, 15 W, 45 min): lane 1: control DNA alone; lane 2: control DNA + DMSO; lane 3: DNA and **4b** (no hυ); lane 4: DNA and **4b**; lane 5: DNA and **4a** (no hυ); lane 6: DNA and **4a**; lane 7: DNA and **4i** (no hυ); lane 8: DNA and **4i**. (b) Effects of different substituents on photocleavage, lane 1: control DNA alone; lane 2: control DNA + DMSO (no hυ); lane 3: control DNA + DMSO; lane 4: DNA and **4j** (no hυ); lane 5: DNA and **4j**; lane 6: DNA and **4k** (no hυ); lane 7: DNA and **4k**.

It is noteworthy that compounds **4j** and **4k** (lane 5, 7, respectively, Fig. 2b) with 2′-thienyl moiety are relatively stronger photocleaver than corresponding oxygen containing counterpart **4i** (lane 8, Fig. 2a) which is in consonance with literature report [41]. Preliminary experiment indicates that the compounds **4a**, **4j** and **4k** acted more efficiently than the other analogues under the identical conditions. Therefore, compounds **4a** and **4k** were chosen to carry out time dependant and concentration dependant studies on photocleavage activity.

Further experiment indicated that with the prolongation of photoirradiation time the cleaving ability of the compounds **4k** and **4a** increased remarkably (Fig. 3a and b), signifying it was a time-dependent process. Control experiment using DNA + DMSO alone (Fig. 3a, lane 2) did not show any significant cleavage of supercoiled DNA even on longer exposure time (90 min) compared to control lane 1. Compounds **4k** and **4a** at concentration of 30 μg and 40 μg, respectively, cleaved plasmid DNA completely to generate much smaller fragments which were invisible on agarose gel (Fig. 3a, lane 8 and Fig. 3b, lane 7) under 90 min photoirradiation. In addition, there were noteworthy cleavage enhancements in the presence of **4a** (40 μg) at all time intervals (lane 3–7) and the observation of complete DNA cleavage after only 60 min of irradiation (lane 6) as shown in Fig. 3b.

To assess the conditions that were optimal for observation of enhance DNA cleavage, we incubated different concentrations of **4k** with supercoiled plasmid DNA for 60 min in the presence of UV. It is evident from Fig. 3c that compound **4k** could damage the supercoiled DNA into the relaxed circular form at concentration as low as 10 μg. It can be seen that when the concentration of the test solution was increased from 10 μg to 15 μg for **4k** a concentration dependent DNA cleavage was observed (compare Fig. 3c and d, lane 3–7). But compound **4k** at higher concentrations (40 μg) could not be examined because of the precipitation of **4k** in the reaction mixture. The observation of concentration dependence is also consistent with **4a,** where incubation of circular DNA with increasing concentration of **4a** from 30 μg to 40 μg resulted in elevated levels of nicked plasmid and the amount of Form I diminished gradually (compare Fig. 3b and e). In contrast, the photocleavage ability of **4k** (15 μg) is remarkably stronger than its analog **4a** (30 μg) at less concentration, who cleaves DNA at less concentration (45–60 min, 312 nm) (Fig. 3d and e). In fact, it was found that compound **4a** and **4k** do not promote complete conversion of Form I to Form II even at a concentration of 30 μg (45 min, 312 nm). Compound **4k** showed the promising photocleavage activity at lower concentration. Notably, cleavage by **4k**, containing 5′-bromo-2′-thienyl attached to triazole ring, was much more efficient than cleavage by **4a**.

Photocleaving abilities of hydrazone derivatives **3a, b**, **i-k** were also examined with pMaxGFP DNA upon irradiation at 312 nm for 45 min, using the same conditions employed for cleavage by **4**, as shown in Fig. 4. It can be seen from results that the intensity of the supercoiled DNA (form I) band was found to decrease with compounds **3a** and **3k** in contrast with other compounds.

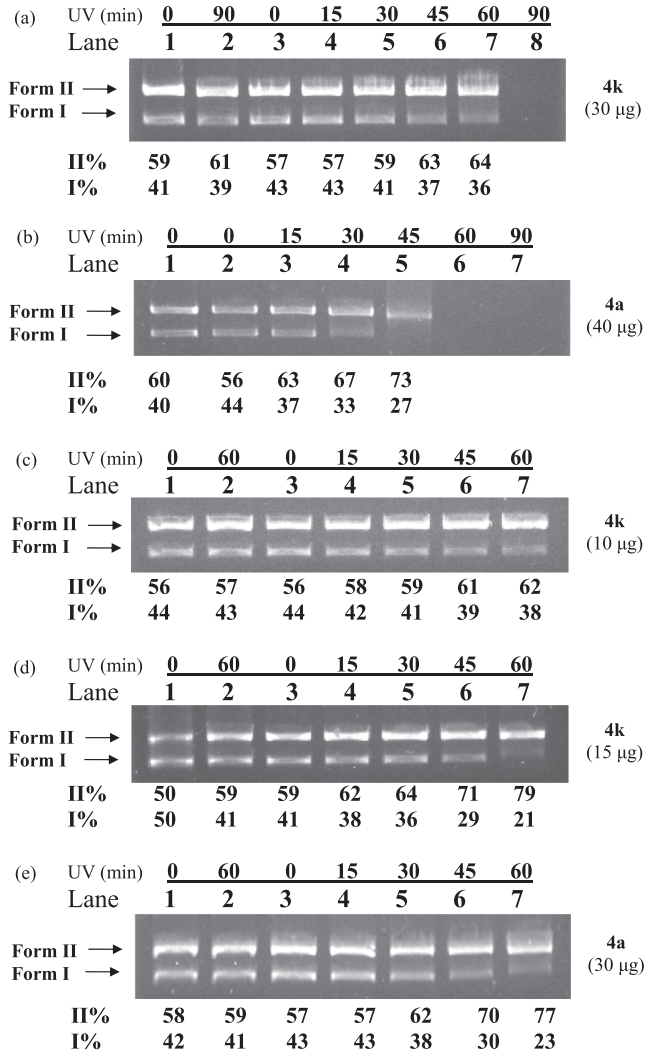


**Fig. 3.** Photocleavage of pMaxGFP DNA (Form I) (0.2 µg/µl) with **4k** and **4a** in Tris-Acetate-EDTA buffer (pH 8.0) under photoirradiation through a transilluminator (312 nm). (a) Photocleavage of DNA by **4k** (30 µg) at various time intervals. Lane 1: control DNA alone (no hυ); lane 2: control DNA + DMSO (hυ, 90 min); lane 3–8: DNA + **4k** at 0, 15, 30, 45, 60, 90 min irradiation, respectively. (b) Time dependence of photocleavage for **4a**. Lane 1: control DNA + DMSO (no hυ); lane 2–7: DNA and **4a** (40 µg) (hυ, 0, 15, 30, 45, 60, 90 min), respectively. (c) Photocleavage of compound **4k**. Lane 1: control DNA alone (no hυ); lane 2: control DNA + DMSO (hυ, 60 min); lane 3–7: DNA + **4k** at the concentration of 10 µg at 0, 15, 30, 45, 60 min irradiation, respectively. (d) Concentration dependent photocleavage of DNA by **4k**. Lane 1: control DNA alone (no hυ); lane 2: control DNA + DMSO (hυ, 60 min); lane 3–7: DNA and **4k** at the concentration of 15 µg at 0, 15, 30, 45, 60 min irradiation, respectively. (e) Concentration dependent photocleavage of DNA by **4a**. Lane 1: control DNA alone (no hυ); lane 2: control DNA + DMSO (hυ, 60 min); lane 3–7: DNA and **4a** at the concentration of 30 µg at 0, 15, 30, 45, 60 min irradiation, respectively.

### 4.3. Mechanistic studies

The mechanistic aspects of the photoinduced pMaxGFP DNA cleavage activity of **4k** were investigated through the use of different additives as potential inhibitors/activator and typical results are shown in Fig. 5. Typically, photocleavage of DNA could proceed *via* a variety of mechanisms involving hydrogen abstraction, electron transfer, reactive oxygen species (ROS) *viz.* hydroxyl radical, superoxide anion radical, and singlet oxygen. Control experiment shows that L-histidine (singlet oxygen quencher) significantly increased the DNA photocleavage activity (lane 3), which indicated that the singlet oxygen ($^1O_2$) (Type II mechanism) may not be involved in the DNA damage. Elimination of

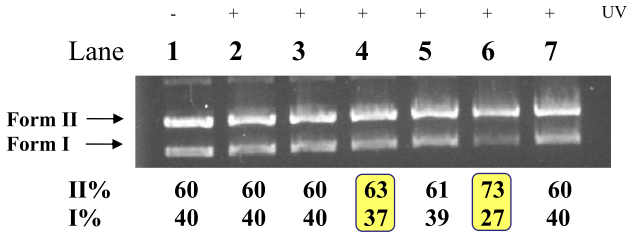


**Fig. 4.** Ethidium bromide stained agarose gel (0.8%) showing light induced cleavage of 200 ng supercoiled circular pMaxGFP plasmid DNA (Form I) to relaxed circular DNA (Form II) by 3 µl of compounds **3a**, **3b**, **3j** (30 µg, stock solution 10 mg/mL) and **3i, 3k** (15 µg, stock solution 5 mg/mL) upon irradiation of UV light (312 nm) in a TAE buffer under aerobic condition at room temperature for 45 min. Lane 1: control DNA alone (no hυ); lane 2: control DNA + DMSO; lane 3: DNA + **3j**; lane 4: DNA + **3k**; lane 5: DNA + **3b**; lane 6: DNA + **3a**; lane 7: DNA + **3i**.

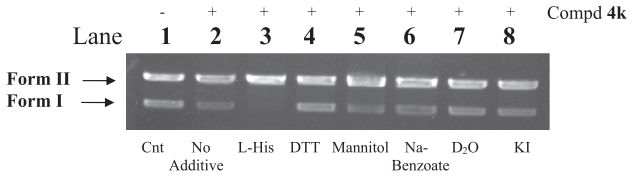


**Fig. 5.** Cleavage of pMaxGFP DNA by compound **4k** (30 µg) on photoirradiation at 312 nm for 45 min in presence of different additives. Lane 1: DNA control; Lane 2: DNA and **4k** (no additive); Lane 3–8: DNA and **4k** in the presence of L-histidine (10 mM), DTT (50 mM), mannitol (50 mM), sodium benzoate (50 mM), $D_2O$ (1 µl), KI (50 mM), respectively.

$^1O_2$ as ROS is further substantiated by another experiment (lane 7) where in activator $D_2O$, a $^1O_2$ enhancer, does not exhibit any enhancement of cleaved supercoiled DNA. Photoirradiation of **4k** in the presence of different hydroxyl radical ($OH^{\cdot}$) scavengers such as mannitol (lane 5) and sodium benzoate (lane 6) showed no apparent inhibition in cleavage of supercoiled DNA, however, in presence of KI (lane 8), another hydroxyl radical scavenger, little inhibition (%) was observed on the cleavage efficiency.

Interestingly, the addition of dithiothreitol (DTT) (lane 4), a good superoxide anion radical scavenger, notably inhibits the potential of **4k** towards photocleavage activity, suggesting that compound **4k** might cleave DNA *via* oxidative pathway (Type I mechanism) and superoxide anion radical ($O_2^{-\cdot}$) is likely to be the primary reactive species responsible for the cleavage of DNA. Thus, it was believed that electron transfer to the molecular oxygen from the photo-excited compound **4k** to form superoxide radical anion plays a major role in the photodamage of DNA besides radicals produced by the C=N bond in triazole ring and/or the C=O bond *via* photo-excited $^3(n–\pi^*)$ and/or $^3(\pi–\pi^*)$ states upon photoirradiation [42]. Yang et al reported that isoquinolino[5,4-*ab*]phenazine derivatives photocleaved DNA through superoxide anion and radical based mechanism [43]. Fig. 6 shows the bar diagram representation of the percentage of cleavage for compound **4k** in presence of additives. Error bars are based upon standard deviation. Higher electron densities of the triazoloquinoxalinone chromophores (Fig. S2, Supporting Information) might be responsible to grant these compounds stronger abilities of transferring electrons, which were from their chromophores to oxygen to form superoxide anions responsible for photocleavage under photo-activation.

## 5. Conclusion

In summary, the present study provides a convenient, superior and environmentally benign protocol for synthesizing new [1,2,4]-triazolo [4,3-*a*]quinoxalin-4(5*H*)-ones in terms of shorter reaction time, increased yields, minimal purification of the products and operational simplicity compared to the conventional methods and illustrates the

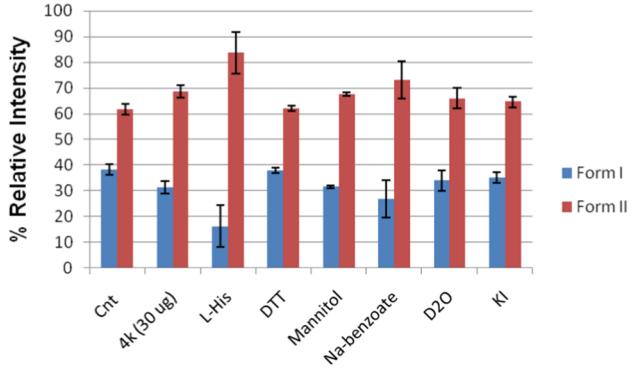


**Fig. 6.** Bar diagram representing the effect of different additives on relative amounts of the two forms of pMaxGFP DNA on photoirradiation in the presence of compound **4k** (30 μg). Reported values reflect the average of three experiments and results are expressed as mean ± S.D. Data were analyzed with Image J software from NIH.

generality and versatility of I(III) as an oxidizing agent. The data from preliminary studies revealed that [1,2,4]-triazolo[4,3-*a*]quinoxalin-4(5*H*)-ones exhibit promising DNA photocleaving activities and the cleavage efficiency was substrate, concentration and time dependent. The mechanism experiments showed that superoxide anion radical (Type I) is mainly responsible for photocleavage. Compound **4k** could be a promising candidate for further photobiological applications such as photodynamic therapeutic and chemotherapeutic.

## 6. Experimental

Melting points were determined in open capillaries using a melting point apparatus and are not corrected. The IR spectra were recorded on a Buck Scientific IR M-500 spectrophotometer in KBr discs ($\nu_{max}$ in $cm^{-1}$). $^1H$ (300 MHz and 400 MHz) and $^{13}C$ NMR (100 MHz) spectra were recorded on a Bruker AV-300 or Bruker AV-400 NMR spectrometer using DMSO-$d_6$ or $CDCl_3$ as a solvent with tetramethylsilane as internal reference. Chemical shifts are reported in parts per million (ppm) and coupling constants $J$ in Hz. High resolution mass spectra (HRMS) were measured in $ESI^+$ mode on a Xevo G2-S QTOF mass spectrometer (Waters, USA) at Materials Research Centre, MNIT, Jaipur, India. The electronic absorption spectra of compounds **4a, b**, **i-k** (dissolved in chloroform to give $10^{-4}$ M solutions) were recorded on a Smart UV-2202 UV–Vis systronics double beam spectrophotometer (700–200 nm) at room temperature. Data were reported in $\lambda_{max}$/nm. 3-Hydrazinoquinoxalin-2(1*H*)-one **2** was prepared according to the literature procedure [36].

### 6.1. General procedure for the synthesis of 3-(2-(aryl/heteroarylidene) hydrazinyl)-quinoxalin-2(1H)-ones (3a-k)

3-Hydrazinoquinoxalin-2(1*H*)-one (**2**) (0.**3 g**, 1.7 mmol) was dissolved in 20 mL ethanol and appropriate aldehyde (1.7 mmol) was added. The reaction mixture was heated under reflux for 2 h and then mixture was allowed to cool at room temperature. The solid residue thus obtained was collected by filteration, dried and recrystallized from ethanol to afford 3-(2-(aryl/heteroarylidene)hydrazinyl)-quinoxalin-2(1*H*)-ones **3**.

#### 6.1.1. (E)-3-(2-(4′-Bromobenzylidene)hydrazinyl)-quinoxalin-2(1H)-one (3d)

IR: 3155 (N−H str), 1682 (C═O), 1620 (C═N); $^1H$ NMR (400 MHz, DMSO-$d_6$) δ: 7.19–7.24 (m, 3H, quinox-5-H, 6-H, 7-H), 7.52–7.54 (dd, 1H, $J_o$ = 8.4 Hz, $J_m$ = 1.76 Hz, quinox-8-H), 7.67 (m, 4H, Ph-3′,5′,2′,6′-H), 8.56 (s, 1H, N═C−H), 11.30 (s, 1H, NH, $D_2O$ exchangeable), 12.41 (s, 1H, amide NH, $D_2O$ exchangeable); $^{13}C$ NMR (100 MHz, DMSO-$d_6$) δ: 115.52, 123.16, 123.98, 125.28, 126.07, 129.14, 129.25, 130.83, 132.08, 132.29, 133.23, 134.54, 145.78, 146.57, 151.26. *Anal.* Calcd. for $C_{15}H_{11}BrN_4O$: C, 52.50; H, 3.23; N, 16.33. Found: C, 52.69; H, 3.53; N, 16.57%.

#### 6.1.2. (E)-3-(2-(4′-Methylbenzylidene)hydrazinyl)-quinoxalin-2(1H)-one (3e)

IR: 3155 (N−H str), 1674 (C═O), 1605 (C═N); $^1H$ NMR (400 MHz, DMSO-$d_6$) δ: 2.35 (s, 3H, 4′-$CH_3$), 7.18–7.22 (m, 3H, quinox-5, 6, 7-H), 7.27–7.29 (d, 2H, $J_o$ = 7.96 Hz, Ph-3′,5′-H), 7.52–7.54 (d, 1H, $J_o$ = 8.24 Hz, quinox-8-H), 7.61–7.63 (d, 2H, $J_o$ = 8.0 Hz, Ph-2′,6′-H), 8.54 (s, 1H, N═C−H), 11.16 (s, 1H, NH, $D_2O$ exchangeable), 12.38 (s, 1H, amide NH, $D_2O$ exchangeable); $^{13}C$ NMR (100 MHz, DMSO-$d_6$) δ: 21.51, 115.49, 123.98, 125.06, 125.92, 127.37, 129.07, 129.12, 129.70, 129.89, 132.51, 133.35, 139.88, 146.57, 147.32, 151.31. *Anal.* Calcd. for $C_{16}H_{14}N_4O$: C, 69.05; H, 5.07; N, 20.13. Found: C, 69.52; H, 5.16; N, 20.38%.

#### 6.1.3. (E)-3-(2-(2′,5′-Dimethoxybenzylidene)hydrazinyl)-quinoxalin-2(1H)-one (3g)

IR: 3194 (N−H str), 1674 (C═O), 1612 (C═N); $^1H$ NMR (400 MHz, DMSO-$d_6$) δ: 3.79 (s, 3H, 5′-$OCH_3$), 3.83 (s, 3H, 2′-$OCH_3$), 6.97–7.01 (dd, 1H, $J_o$ = 9.42 Hz, $J_m$ = 2.96 Hz, Ph-4′-H), 7.03–7.06 (m, 2H, Ph-3′-H, quinox-5-H), 7.18–7.21 (m, 2H, quinox-6, 7-H), 7.44–7.45 (d, 1H, $J_m$ = 2.84 Hz, Ph-5′-H), 7.51–7.53 (d, 1H, $J_o$ = 6.92 Hz, quinox-8-H), 8.87 (s, 1H, N═C−H), 11.30 (s, 1H, NH, $D_2O$ exchangeable), 12.36 (s, 1H, amide NH, $D_2O$ exchangeable); $^{13}C$ NMR (100 MHz, DMSO-$d_6$) δ: (*E-Z* mixture) 56.01, 56.12, 56.49, 56.83, 110.42, 112.57, 113.64, 113.85, 115.45, 117.06, 118.30, 122.24, 123.41, 123.89, 124.25, 125.05, 125.98, 126.45, 129.20, 133.30, 142.70, 145.76, 146.65, 151.26, 152.59, 152.83, 153.39, 153.75, 155.29. *Anal.* Calcd. for $C_{17}H_{16}N_4O_3$: C, 62.95; H, 4.97; N, 17.27. Found: C, 62.62; H, 4.69; N, 17.45%.

#### 6.1.4. (E)-3-(2-(3′,4′-Dimethoxybenzylidene)hydrazinyl)-quinoxalin-2(1H)-one (3h)

IR: 3248 (N−H str), 1674 (C═O), 1612 (C═N); $^1H$ NMR (400 MHz, DMSO-$d_6$) δ: 3.82 (s, 3H, 4′-$OCH_3$), 3.85 (s, 3H, 3′-$OCH_3$), 7.03–7.06 (m, 2H, quinox-5-H, Ph-5′-H), 7.18–7.21 (m, 3H, quinox-6, 7-H, Ph-6′-H), 7.34 (m, 1H, Ph-2′-H), 7.51–7.52 (m, 1H, quinox-8-H), 8.50 (s, 1H, N═C−H), 11.07 (s, 1H, NH, $D_2O$ exchangeable), 12.37 (s, 1H, amide NH, $D_2O$ exchangeable); $^{13}C$ NMR (100 MHz, DMSO-$d_6$) δ: 56.06, 56.1, 109.15, 112.10, 115.46, 121.78, 123.92, 124.89, 125.87, 127.99, 129.08, 133.40, 146.49, 147.54, 149.51, 150.94, 151.33. *Anal.* Calcd. for $C_{17}H_{16}N_4O_3$: C, 62.95; H, 4.97; N, 17.27. Found: C, 63.12; H, 4.81; N, 17.63%.

#### 6.1.5. (E)-3-(2-(Thiophen-2′-ylmethylidene)hydrazinyl)-quinoxalin-2(1H)-one (3j)

IR: 3297 (N−H str), 1674 (C═O), 1612 (C═N); $^1H$ NMR (300 MHz, DMSO-$d_6$) δ: 7.12–7.15 (d, 1H, $J_o$ = 8.1 Hz, quinox-5-H), 7.20–7.21 (m, 3H, quinox-6, 7, 8-H), 7.37–7.38 (d, 1H, $J_{3′,\ 4′}$ = 2.7 Hz, thiophene-3′-H) 7.51–7.53 (d, 1H, $J_{4′,\ 5′}$ = 5.1 Hz, thiophene-4′-H), 7.63–7.65 (d, 1H, $J_{4′,\ 5′}$ = 4.8 Hz, thiophene-5′-H), 8.78 (s, 1H, N═C−H), 11.24 (s, 1H, NH, $D_2O$ exchangeable), 12.40 (s, 1H, amide NH, $D_2O$ exchangeable); $^{13}C$ NMR (100 MHz, DMSO-$d_6$) δ: 115.12, 123.65, 124.59, 125.57, 127.78, 128.36, 128.56, 130.01, 132.76, 139.48, 141.27, 146.03, 150.92. HRMS: *m/z* 271.0657 $[M + 1]^+$ ($C_{13}H_{10}N_4OS$ $[M + 1]^+$ requires 271.0653). *Anal.* Calcd. for $C_{13}H_{10}N_4OS$: C, 57.76; H, 3.73; N, 20.73. Found: C, 57.82; H, 3.61; N, 20.92%.

#### 6.1.6. (E)-3-(2-(5′-Bromothiophen-2′-ylmethylidene)hydrazinyl)-quinoxalin-2(1H)-one (3k)

IR: 3155 (N−H str), 1674 (C═O), 1605 (C═N); $^1H$ NMR (400 MHz, DMSO-$d_6$) δ: 7.09–7.32 (m, 5H, thiophene-3′-H, quinox-5, 6, 7, 8-H), 7.51–7.52 (d, 1H, $J_{4′,\ 5′}$ = 5.1 Hz, thiophene-4′-H), 8.77 (s, 1H,

N═C−H), 11.37 (s, 1H, NH, $D_2O$ exchangeable), 12.33 (s, 1H, amide NH, $D_2O$ exchangeable); $^{13}C$ NMR (100 MHz, DMSO-$d_6$) δ: 115.51, 116.81, 123.92, 124.25, 126.06, 128.91, 129.14, 131.75, 133.00, 142.02, 146.21, 147.51, 151.21. *Anal.* Calcd. for $C_{13}H_9BrN_4OS$: C, 44.71; H, 2.60; N, 16.04. Found: C, 44.82; H, 2.81; N, 16.42%.

### 6.2. General procedure for cyclization of hydrazones (**3a-k**) to 1-aryl/heteroaryl-[1,2,4]-triazolo[4,3-a]quinoxalin-4(5H)-ones (**4a-k**)

To a stirred suspension (or) solution of hydrazone (**3**) (1.0 mmol) in dichloromethane (20 mL) was added IBD (0.354 g, 1.1 mmol) in small portions over a period of five minutes at room temperature. The reaction mixture was allowed to stir for about 2 h or till the completion of reaction as monitored by TLC. Excess of dichloromethane was distilled off in vacuo and the residual mass was triturated with petroleum ether to give solid product which was recrystallized from ethanol.

#### 6.2.1. 1-(4′-Bromophenyl)-[1,2,4]-triazolo[4,3-a]quinoxalin-4(5H)-one (**4d**)

IR: 1682 (C═O), 1612 (C═N); $^1H$ NMR (400 MHz, DMSO-$d_6$) δ: 7.05–7.12 (m, 2H, quinox-6-H, 7-H), 7.37–7.42 (m, 2H, quinox-5-H, 8-H), 7.69–7.72 (td, 2H, $J_o$ = 8.56, $J_p$ = 1.96, $J_m$ = 2.36, Ph-3′, 5′-H), 7.88–7.91 (td, 2H, $J_o$ = 8.56, $J_m$ = 2.32, $J_p$ = 1.96, Ph-2′, 6′-H), 12.12 (s, 1H, amide NH, $D_2O$ exchangeable); $^{13}C$ NMR (100 MHz, DMSO-$d_6$) δ: 116.70, 117.67, 121.25, 123.23, 125.19, 127.87, 128.26, 129.89, 132.44, 132.74, 144.90, 150.24, 152.33. HRMS: *m/z* 340.9970 $[M + 1]^+$, 342.9951 $[M + 1 + 2]^+$ in the ratio showing typical bromine isotope profile (1:1), ($C_{15}H_9BrN_4O$ $[M + 1]^+$ requires 341.0038). *Anal.* Calcd. for $C_{15}H_9BrN_4O$: C, 52.81; H, 2.66; N, 16.42. Found: C, 53.03; H, 2.88; N, 16.18%.

#### 6.2.2. 1-(4′-Methylphenyl)-[1,2,4]-triazolo[4,3-a]quinoxalin-4(5H)-one (**4e**)

IR: 1682 (C═O), 1612 (C═N); $^1H$ NMR (400 MHz, DMSO-$d_6$) δ: 2.48 (s, 3H, 4′-$CH_3$), 7.00–7.05 (dt, 1H, $J_o$ = 8.56 Hz, $J_m$ = 2.08 Hz, quinox-6-H), 7.11–7.13 (d, 1H, $J_o$ = 8.08 Hz, quinox-7-H), 7.35–7.42 (m, 2H, quinox-5, 8-H), 7.47–7.49 (d, 2H, $J_o$ = 7.88 Hz, Ph-3′, 5′-H), 7.60–7.62 (d, 2H, $J_o$ = 8.04 Hz, Ph-2′, 6′-H), 12.10 (s, 1H, amide NH, $D_2O$ exchangeable); $^{13}C$ NMR (100 MHz, DMSO-$d_6$) δ: 21.61, 116.56, 117.63, 121.37, 123.03, 125.67, 126.95, 128.16, 129.44, 129.90, 130.20, 141.25, 144.71, 151.20, 152.41. HRMS: *m/z* 277.1083 $[M + 1]^+$, 278.1106 $[M + 2]^+$ ($C_{16}H_{12}N_4O$ $[M + 1]^+$ requires 277.1089). *Anal.* Calcd. for $C_{16}H_{12}N_4O$: C, 69.55; H, 4.38; N, 20.28. Found: C, 69.72; H, 4.61; N, 20.57%.

#### 6.2.3. 1-(2′,5′-Dimethoxyphenyl)-[1,2,4]-triazolo[4,3-a]quinoxalin-4(5H)-one (**4g**)

IR: 1682 (C═O), 1612 (C═N); $^1H$ NMR (400 MHz, DMSO-$d_6$) δ: 3.60 (s, 3H, 2′-$OCH_3$), 3.79 (s, 3H, 5′-$OCH_3$), 7.06–7.08 (m, 2H, quinox-6, 7-H), 7.17–7.18 (d, 1H, $J_m$ = 2.92 Hz, Ph-6′-H), 7.23–7.25 (d, 1H, $J_o$ = 9.04 Hz, Ph-3′-H), 7.28–7.31 (dd, 1H, $J_o$ = 9.12 Hz, $J_m$ = 3.0 Hz, Ph-4′-H), 7.40–7.42 (m, 2H, quinox-5, 8-H), 12.14 (s, 1H, amide NH, $D_2O$ exchangeable); $^{13}C$ NMR (100 MHz, DMSO-$d_6$) δ: 56.20, 56.48, 113.64, 116.14, 117.31, 117.49, 117.87, 118.49, 121.25, 123.37, 128.33, 129.55, 144.57, 148.35, 152.04, 152.23, 153.72. HRMS: *m/z* 323.1067 $[M + 1]^+$, 324.1095 $[M + 2]^+$ ($C_{17}H_{14}N_4O_3$ $[M + 1]^+$ requires 323.1144). *Anal.* Calcd. for $C_{17}H_{14}N_4O_3$: C, 63.35; H, 4.38; N, 17.38. Found: C, 63.69; H, 4.03; N, 17.81%.

#### 6.2.4. 1-(3′,4′-Dimethoxyphenyl)-[1,2,4]-triazolo[4,3-a]quinoxalin-4(5H)-one (**4h**)

IR: 1682 (C═O), 1620 (C═N); $^1H$ NMR (400 MHz, DMSO-$d_6$) δ: 3.76 (s, 3H, 4′-$OCH_3$), 3.90 (s, 3H, 3′-$OCH_3$), 7.05–7.09 (dt, 1H, $J_o$ = 8.6 Hz, $J_m$ = 2.32 Hz, quinox-6-H), 7.17–7.19 (d, 1H, $J_o$ = 8.12 Hz, quinox-7-H), 7.21–7.24 (d, 1H, $J_o$ = 8.28 Hz, Ph-5′-H), 7.26–7.28 (dd, 1H, $J_o$ = 8.2 Hz, $J_m$ = 1.84 Hz, Ph-6′-H), 7.30–7.31 (d, 1H, $J_m$ = 1.84 Hz, Ph-2′-H), 7.38–7.42 (m, 2H, quinox-5, 8-H), 12.08 (s, 1H, amide NH, $D_2O$ exchangeable); $^{13}C$ NMR (100 MHz, DMSO-$d_6$) δ: 56.13, 56.24, 112.44, 113.55, 116.79, 117.57, 120.36, 121.42, 123.11, 123.22, 128.15, 129.87, 144.55, 149.40, 151.19, 152.39. HRMS: *m/z* 323.1132 $[M + 1]^+$, 324.1159 $[M + 2]^+$ ($C_{17}H_{14}N_4O_3$ $[M + 1]^+$ requires 323.1144). *Anal.* Calcd. for $C_{17}H_{14}N_4O_3$: C, 63.35; H, 4.38; N, 17.38. Found: C, 63.21; H, 4.66; N, 17.77%.

#### 6.2.5. 1-(Thiophen-2′-yl)-[1,2,4]-triazolo[4,3-a]quinoxalin-4(5H)-one (**4j**)

IR: 3140 (N−H str), 1682 (C═O), 1612 (C═N); $^1H$ NMR (300 MHz, DMSO-$d_6$) δ: 7.06–7.11 (t, 1H, $J_o$ = 8.4 Hz, quinox-6-H), 7.22–7.25 (d, 1H, $J_o$ = 8.4 Hz, quinox-7-H), 7.38–7.39 (dd, 1H, $J_{5',4'}$ = 5.1 Hz, $J_{3',4'}$ = 3.9 Hz, thiophene-4′-H), 7.39–7.43 (m, 2H, quinox-5, 8-H), 7.64–7.66 (d, 1H, $J_{3',4'}$ = 3.3 Hz, thiophene-3′-H), 8.04–8.06 (d, 1H, $J_{4',5'}$ = 5.1 Hz, thiophene-5′-H), 12.12 (s, 1H, amide NH, $D_2O$ exchangeable); $^{13}C$ NMR (100 MHz, DMSO-$d_6$) δ: 116.35, 117.65, 121.27, 123.18, 127.25, 128.42, 128.69, 129.97, 131.68, 132.60, 145.20, 145.43, 152.21. HRMS: *m/z* 269.0501 $[M + 1]^+$ ($C_{13}H_8N_4OS$ $[M + 1]^+$ requires 269.0497). *Anal.* Calcd. for $C_{13}H_8N_4OS$: C, 58.20; H, 3.01; N, 20.88. Found: C, 57.92; H, 3.15; N, 20.92%.

#### 6.2.6. 1-(5′-Bromothiophen-2′-yl)-[1,2,4]-triazolo[4,3-a]quinoxalin-4(5H)-one (**4k**)

IR: 1680 (C═O), 1612 (C═N); $^1H$ NMR (300 MHz, $CDCl_3$) δ: 6.87–6.89 (d, 1H, $J_o$ = 8.1 Hz, quinox-6-H), 6.92–6.95 (m, 1H, quinox-7-H), 7.10–7.15 (m, 2H, thiophene-4′, 3′-H), 7.17–7.20 (d, 1H, $J_o$ = 7.8 Hz, quinox-5-H), 7.33–7.36 (d, 1H, $J_o$ = 8.7 Hz, quinox-8-H), 12.09 (s, 1H, amide NH, $D_2O$ exchangeable); $^{13}C$ NMR (100 MHz, DMSO-$d_6$) δ: 115.63, 116.21, 118.00, 123.25, 123.40, 125.42, 128.43, 129.46, 130.82, 132.09, 144.97, 148.03, 152.71. *Anal.* Calcd. for $C_{13}H_7BrN_4OS$: C, 44.97; H, 2.03; N, 16.14. Found: C, 45.29; H, 2.43; N, 16.45%.

## 7. Biological activity

### 7.1. Material

The DMSO, ethylenediaminetetraacetic acid (EDTA) and ethidium bromide (EtBr) were purchased from Sigma-Aldrich, USA. pMaxGFP plasmid was obtained from Lonza. Stock solutions of compound **4** (15 mg/mL) and **3a**, **3b**, **3j** (10 mg/mL) and **3i, 3k** (5 mg/mL) were prepared in DMSO and stored in brown containers in the refrigerator. All gel electrophoresis experiments were performed in 1 × TAE buffer (0.04 M Tris-borate, 0.114% acetic acid and 50 mM EDTA, pH 8.0). Quantification of cleavage efficiency was performed by integration of the optical density as a function of the band area using the Image J Software (recommended by NIH, USA) [44].

### 7.2. DNA photocleavage assays

The DNA photoactivated cleavage experiments were performed by treating 0.2 μg/μl of supercoiled pMaxGFP plasmid (Lonza) DNA in the TAE buffer with the compound **4** or **3** (presence/absence) dissolved in DMSO at room temperature and the solution was then irradiated at ambient atmospheric pressure under aerobic condition for the indicated time using a UV-lamp (312 nm, 15 W). Reactions were also performed without irradiation as control. After illumination all reactions were quenched by adding 2 μl of 6 × gel loading dye (containing 0.25% bromophenol blue in 30% glycerol) in TAE buffer. Cleavage products were electrophoresed for 45–60 min in TAE buffer at 120 V on a 0.8% agarose gel by using BioRad electrophoresis system. The nicked and supercoiled forms of pMaxGFP plasmid DNA were then visualized by staining the gel with fluorescent and DNA intercalating dye i.e. ethidium bromide (0.5 μg/mL). The gel was washed with water and DNA bands were visualized and photographed on a ChemiDoc XRS + CCD

camera (BioRad) with fluorescence chemiluminescence and visible imaging system. Amounts of supercoiled (form I) and nicked DNA (form II) were then quantified from the intensities of the bands using Image J software. In order to identify ROS responsible for DNA cleavage, control experiments were performed using several additives as potential inhibitors/activator that was added to supercoiled DNA prior to the addition of compounds. L-Histidine (10 mM) was used as $^1O_2$ quencher, DTT (50 mM) was used as a $O_2^{-\cdot}$ quencher, mannitol (50 mM), sodium benzoate (50 mM) and KI (50 mM) were used as $OH^{\cdot}$ scavengers.

## Acknowledgements

We are thankful to Sophisticated Analytical Instrument Facility, Central Drug Research Institute, Lucknow, India for providing elemental analyses. Thanks are also due to Prof. Devinder Kumar, Department of Chemistry and Dr. APJ Abdul Kalam Central Instrumentation Laboratory, Guru Jambheshwar University of Science & Technology, Hisar for providing NMR data. Support of this research by D. A. V. College (Lahore), Ambala City in providing infrastructure and lab facility is gratefully acknowledged.

## Appendix A. Supplementary material

Supplementary data to this article can be found online at https://doi.org/10.1016/j.bioorg.2019.102932.

## References

[1] K. Gurova, New hopes from old drugs: revisiting DNA-binding small molecules as anticancer agents, Future Oncol. 5 (2009) 1685–1704.
[2] S. Gowda KR, B.B. Mathew, C.N. Sudhamani, H.S.B. Naik, Mechanism of DNA binding and cleavage, Biomed. Biotechnol. 2 (2014) 1–9.
[3] A. Ali, S. Bhattacharya, DNA binders in clinical trials and chemotherapy, Bioorg. Med. Chem. 22 (2014) 4506–4521.
[4] R. Martinez, L. Chacon-Garcia, The search of DNA-intercalators as antitumoral drugs: what it worked and what did not work, Curr. Med. Chem. 12 (2005) 127–151.
[5] B. Armitage, Photocleavage of nucleic acids, Chem. Rev. 98 (1998) 1171–1200.
[6] S. Monti, I. Manet, Supramolecular photochemistry of drugs in biomolecular environments, Chem. Soc. Rev. 43 (2014) 4051–4067.
[7] S.M. Touami, C.C. Poon, P.A. Wender, Sequence specific DNA cleavage by conjugates of benzotriazoles and minor groove binders, J. Am. Chem. Soc. 119 (1997) 7611–7612.
[8] B. Breiner, J.C. Schlatterer, S.V. Kovalenko, N.L. Greenbaum, I.V. Alabugin, Protected $^{32}$P-labels in deoxyribonucleotides: investigation of sequence selectivity of DNA photocleavage by enediyne-, fulvene-, and acetylene-lysine conjugates, Angew. Chem. Int. Ed. 45 (2006) 3666–3670.
[9] S. Lindemose, P.E. Nielsen, M. Hansen, N.E. Mollegaard, A DNA minor groove electronegative potential genome map based on photo-chemical probing, Nucleic Acids Res. 39 (2011) 6269–6276.
[10] S. Banerjee, E.B. Veale, C.M. Phelan, S.A. Murphy, G.M. Tocci, L.J. Gillespie, D.O. Frimannsson, J.M. Kelly, T. Gunnlaugsson, Recent advances in the development of 1,8-naphthalimide based DNA targeting binders, anticancer and fluorescent cellular imaging agents, Chem. Soc. Rev. 42 (2013) 1601–1618.
[11] B. Armitage, G.B. Schuster, Anthraquinone photonucleases: A surprising role for chloride in the sequence-neutral cleavage of DNA and the footprinting of minor groove-bound ligands, Photochem. Photobiol. 66 (1997) 164–170.
[12] M.-P. Teulade-Fichou, D. Perrin, A. Boutorine, D. Polverari, J.-P. Vigneron, J.-M. Lehn, J.-S. Sun, T. Garestier, C. Hélène, Direct photocleavage of HIV-DNA by quinacridine derivatives triggered by triplex formation, J. Am. Chem. Soc. 123 (2001) 9283–9292.
[13] M. Bio, P. Rajaputra, G. Nkepang, S.G. Awuah, A.M.L. Hossion, Y. You, Site-specific and far-red-light-activatable prodrug of combretastatin A-4 using photo-unclick chemistry, J. Med. Chem. 56 (2013) 3936–3942.
[14] R. Adam, P. Bilbao-Ramos, B. Abarca, R. Ballesteros, M.E. González-Rosende, M.A. Dea-Ayuela, F. Estevan, G. Alzuet-Piña, Triazolopyridopyrimidines: an emerging family of effective DNA photocleavers. DNA binding. Antileishmanial activity, Org. Biomol. Chem. 13 (2015) 4903–4917.
[15] M. Pasolli, K. Dafnopoulos, N.-P. Andreou, P.S. Gritzapis, M. Koffa, A.E. Koumbis, G. Psomas, K.C. Fylaktakidou, Pyridine and p-nitrophenyl oxime esters with possible photochemotherapeutic activity: synthesis, DNA photocleavage and DNA binding studies, Molecules 21 (2016) 864, https://doi.org/10.3390/molecules21070864.
[16] R. Weijer, M. Broekgaarden, M. Kos, R. van Vught, E.A.J. Rauws, E. Breukink, T.M. van Gulik, G. Storm, M. Heger, Enhancing photodynamic therapy of refractory solid cancers: combining second-generation photosensitizers with multi-targeted liposomal delivery, J. Photochem. Photobiol. C 23 (2015) 103–131.
[17] J. Kou, D. Dou, L. Yang, Porphyrin photosensitizers in photodynamic therapy and its applications, Oncotarget 8 (2017) 81591–81603.
[18] J. Zhang, C. Jiang, J.P.F. Longo, R.B. Azevedo, H. Zhang, L.A. Muehlmann, An updated overview on the development of new photosensitizers for anticancer photodynamic therapy, Acta Pharm. Sin. B 8 (2018) 137–146.
[19] L.M. Wilhelmsson, N. Kingi, J. Bergman, Interactions of antiviral indolo[2,3-*b*]quinoxaline derivatives with DNA, J. Med. Chem. 51 (2008) 7744–7750.
[20] M.K. Ibrahim, M.S. Taghour, A.M. Metwaly, A. Belal, A.B.M. Mehany, M.A. Elhendawy, M.M. Radwan, A.M. Yassin, N.M. El-Deeb, E.E. Hafez, M.A. ElSohly, I.H. Eissa, Design, synthesis, molecular modeling and anti-proliferative evaluation of novel quinoxaline derivatives as potential DNA intercalators and topoisomerase II inhibitors, Eur. J. Med. Chem. 155 (2018) 117–134.
[21] W. Szczepanik, M. Kucharczyk-Klaminska, P. Stefanowicz, A. Staszewska, Z. Szewczuk, J. Skała, A. Mysiak, M. Jezowska-Bojczuk, DNA oxidative cleavage induced by the novel peptide derivatives of 3-(quinoxalin-6-yl)alanine in combination with Cu(II) or Fe(II) Ions, Bioinorg. Chem. Appl. (2009) 906836, https://doi.org/10.1155/2009/906836.
[22] X. Li, Y. Lin, Q. Wang, Y. Yuan, H. Zhang, X. Qian, The novel anti-tumor agents of 4-triazol-1,8-naphthalimides: Synthesis, cytotoxicity, DNA intercalation and photocleavage, Eur. J. Med. Chem. 46 (2011) 1274–1279.
[23] J.W. Yang, P.A. Wender, Synthesis of 1-(2-naphthoyl) benzotriazoles as photoactivated DNA cleaving agents, Arch. Pharm. Res. 20 (1997) 197–199.
[24] P.A. Wender, S.M. Touami, C. Alayrac, U.C. Philipp, Triazole photonucleases: a new family of light activatable DNA cleaving agents, J. Am. Chem. Soc. 118 (1996) 6522–6523.
[25] D.D. Li, J.L. Tian, W. Gu, X. Liu, S.P. Yan, A novel 1,2,4-triazole-based copper(II) complex: Synthesis, characterization, magnetic property and nuclease activity, J. Inorg. Biochem. 104 (2010) 171–179.
[26] R. Aggarwal, G. Sumran, V. Kumar, A. Mittal, Copper(II) chloride mediated synthesis and DNA photocleavage activity of 1-aryl/heteroaryl-4-substituted-1,2,4-triazolo[4,3-*a*]quinoxalines, Eur. J. Med. Chem. 46 (2011) 6083–6088.
[27] S.A. Galal, A.S. Abdelsamie, S.M. Soliman, J. Mortier, G. Wolber, M.M. Ali, H. Tokuda, N. Suzuki, A. Lida, R.A. Ramadan, H.I. El Diwani, Design, synthesis and structure-activity relationship of novel quinoxaline derivatives as cancer chemopreventive agent by inhibition of tyrosine kinase receptor, Eur. J. Med. Chem. 69 (2013) 115–124.
[28] P. Bhattacharya, K. Roy, QSAR of adenosine $A_3$ receptor antagonist 1,2,4-triazolo [4,3-*a*]quinoxalin-1-one derivatives using chemometric tools, Bioorg. Med. Chem. Lett. 15 (2005) 3737–3743.
[29] H. Abul-Khair, S. Elmeligie, A. Bayoumi, A. Ghiaty, A. El-Morsy, M.H. Hassan, Synthesis and evaluation of some new (1,2,4)triazolo(4,3-*a*)quinoxalin-4(5*H*)-one derivatives as AMPA receptor antagonists, J. Heterocycl. Chem. 50 (2013) 1202–1208.
[30] F.A.S. Alasmary, F.S. Alnahdi, A.B. Bacha, A.M. El-Araby, N. Moubayed, A.M. Alafeefy, M.E. El-Araby, New quinoxalinone inhibitors targeting secreted phospholipase A2 and α-glucosidase, J. Enzyme Inhib. Med. Chem. 32 (2017) 1143–1151.
[31] M.M. Badran, K.A.M. Abouzid, M.H.M. Hussein, Synthesis of certain substituted quinoxalines as antimicrobial agents (Part II), Arch. Pharm. Res. 26 (2003) 107–113.
[32] G. Sumran, R. Aggarwal, M. Hooda, D. Sanz, R.M. Claramunt, Unusual synthesis of azines and their oxidative degradation to carboxylic acid using iodobenzene diacetate, Synth. Commun. 48 (2018) 439–446.
[33] R. Aggarwal, C. Rani, G. Sumran, Efficient synthesis of some new 2,3-dimethylquinoxaline-1-oxides using bis(acetoxy)phenyl-$\lambda^3$-iodane as an oxidant, Synth. Commun. 44 (2014) 923–928.
[34] R. Aggarwal, G. Sumran, A. Saini, S.P. Singh, Hypervalent iodine oxidation of benzil-α-arylimino oximes: an efficient synthesis of 2,3-diphenylquinoxaline-1-oxides, Tetrahedron Lett. 47 (2006) 4969–4971.
[35] S. Dong, P.P. Fu, R.N. Shirsat, H.-M. Hwang, J. Leszczynski, H. Yu, UVA light-induced DNA cleavage by isomeric methylbenz[*a*]anthracenes, Chem. Res. Toxicol. 15 (2002) 400–407.
[36] G.W.H. Cheeseman, M. Rafiq, Quinoxalines and related Compounds. Part VIII. The reactions of quinoxaline-2(1*H*)-ones and -2,3(1*H*,4*H*)-diones with hydrazine, J. Chem. Soc. C (1971) 452–454.
[37] N. Rashed, A.M. El Massry, E.S.H. El Ashry, A. Amer, H. Zimmer, A facile synthesis of novel triazoloquinoxalinones and triazinoquinoxalinones, J. Heterocycl. Chem. 27 (1990) 691–694.
[38] O.O. Ajani, O.C. Nwinyi, Synthesis and evaluation of antimicrobial activity of phenyl and furan-2-yl[1,2,4]triazolo[4,3-*a*]quinoxalin-4(5*H*)-one and their hydrazone precursors, Can. J. Pure Appl. Sci. 3 (2009) 983–992.
[39] R. Benassi, A. Benedetti, F. Taddei, R. Cappelletti, D. Nardi, A. Tajana, Conformational analysis of hydrazones. $^1$H dynamic nuclear magnetic resonance and solvent effects in aryl- and 2-furylaldehyde ethylaminoacetylhydrazones, Org. Magn. Reson. 20 (1982) 26–30.
[40] D. Horst, W.P. Burmeister, I.G.J. Boer, D. van Leeuwen, M. Buisson, A.E. Gorbalenya, E.J.H.J. Wiertz, M.E. Ressing, The "Bridge" in the Epstein-Barr virus alkaline exonuclease protein BGLF5 contributes to shutoff activity during productive infection, J. Virol. 86 (2012) 9175–9187.
[41] X. Qian, T.-B. Huang, D.-Z. Wei, D.-H. Zhu, M.-C. Fan, W. Yao, Interaction of naphthyl heterocycles with DNA: effects of thiono and thio groups, J. Chem. Soc., Perkin Trans. 2 (2000) 715–718.
[42] Z. Li, Q. Yang, X. Qian, Novel heterocyclic family of phenyl naphthothiazole carboxamides derived from naphthalimides: synthesis, antitumor evaluation, and DNA photocleavage, Bioorg. Med. Chem. 13 (2005) 3149–3155.
[43] P. Yang, Q. Yang, X. Qian, J. Cui, Novel synthetic isoquinolino[5,4-*ab*]phenazines: Inhibition toward topoisomerase I, antitumor and DNA photo-cleaving activities, Bioorg. Med. Chem. 13 (2005) 5909–5914.
[44] Image J; version 1.50.I. Available online: http://rsb.info.nih.gov/ij/download.html.